

Research Article

Design and Manufacturing of Rotating Bending Fatigue Test Machine

Mustafa ÇİPİL¹, Filiz KARABUDAK², Hamid ZAMANLOU^{3*}

¹ Gumushane University, Faculty of Engineering and Natural Sciences, Department of Mechanical Engineering, 29100, Gumushane, Orcid ID: <https://orcid.org/0009-0007-0483-0860>, E-mail: mustafacipli@gmail.com

² Gumushane University, Faculty of Engineering and Natural Sciences, Department of Mechanical Engineering, 29100, Gumushane, Orcid ID: <https://orcid.org/0000-0002-7365-0333>, E-mail: filizkarabudak@gumushane.edu.tr

³ Ataturk University, Faculty of Engineering, Department of Mechanical Engineering, 25000, Erzurum, Orcid ID: <https://orcid.org/0000-0002-9780-8924>, E-mail: zamanloohamid@gmail.com

* Correspondence: zamanloohamid@gmail.com; Tel.: (+905373375033)

Received 06 December 2023

Received in revised form 21 February 2024

In final form 18 April 2024

Reference: Çipil, M., Karabudak., F., Zamanlou, H. Design and Manufacturing of Rotating Bending Fatigue Test Machine. The European Journal of Research and Development, 4(2), 77-95.

Abstract

Fatigue strength is an important criterion for all materials used. In the past years, it has been observed that materials cannot carry the loads they carry statically under service conditions. This situation is explained by the phenomenon of "cyclic loading" in the literature. Cyclic loadings cause damage by creating a crack in the surface of the material or by exploiting an existing discontinuity. There are many test methods and devices for determining fatigue strength. All of these are based on the repetition of a certain load in different ways. Among the tests applied, the least costly and simplest method is the rotating bending fatigue test.

In this study, a rotating bending fatigue test device was designed and manufactured. Fatigue life of AA 6063 aluminum alloys, which were prepared according to the fatigue test sample standards and with specific properties, were subjected to fatigue test and calculated.

Keywords: Rotational bending fatigue device, Manufacturing, Design, Fatigue

1. Introduction

It is very important to know in advance the strength of metal and aluminum parts exposed to stresses of varying intensity and/or direction. In application areas, mechanical equipment is affected by forces that vary in size and direction, regular and/or irregular, and bending and torsion moments (Swanson, 1974). The decrease in strength of metals caused by repeatedly repeated loading and removal of the load or exposure to stresses of varying direction is called fatigue. These varying forces may cause machine elements and equipment to break well below the yield limit. These fractures, which are frequently encountered today, are called fatigue fractures (Orowan, 1939).

Since fatigue fracture is a brittle fracture phenomenon, it is very difficult to predict where and when the fracture will occur. For example, the strands on the upper side of the cylindrical shaft, which is forced to bend under a static load, constantly try to press, and the strands on the lower side try to pull. As the shaft continues to rotate, the filaments of the material will be exposed to stresses that change periodically between positive and negative values, that is, fully variable strains (Swanson, 1974). These periodically changing stresses cause wear and separation at the grain boundaries of machinery equipment. Generally, the breakage starts from a defect in the internal structure of the material or a weak point on the surface. Around this point, the machine element first gets tired and cracks begin to form. These cracks, which form over time, gradually deepen, and eventually, when the stress in the area outside the crack exceeds the strength of the material, a sudden fracture occurs (Tauscher, 1983).

The first studies on fatigue strength entered the literature with the research carried out by the German scientist August Wöhler between 1850 and 1870 (Marzoli et al. 2006). Wöhler examined the train accident that occurred in Versailles, France, in 1842 and observed that this accident was caused by the breakage of the locomotive axle exposed to repeated cyclic stresses. Wöhler drew the Wöhler curve to apply repeated loads to the axles in locomotives and to characterize the relationship between the load level and the number of repeated cycles (Tauscher, 1983). In subsequent studies, the effects of various factors such as the structure and shape of the materials, the heat treatment applied and the usage environment affecting the fatigue strength were examined.

The first studies on the structure of metals in this field were made by Ewing and Humfrey in 1903 (Ewing and Humfrey, 1903). In the early 1920s, the fatigue strength of metals and metal alloys depending on temperature and corrosion were examined. Mc., who carried out one of the greatest studies in this field. Adam examined the fatigue strength of carbon

steels and cast irons at different temperatures (McAdam, 1927). In 1950, Teed and his colleagues investigated the effects of ambient temperature on metals and their alloys (Teed, 1950). In 1958, Thompson used electron microscopy in his studies on fatigue and it was found that fatigue cracks resulted from shear stresses occurring on the surface of the material (Thompson, 1958). In 1991, Topuz and Uçan conducted studies on crack propagation and fatigue fracture of 36Mn5 alloy steel casting and used the rotational bending fatigue test in their studies. (Uçan and Topuz, 1991).

Yeşildal et al., in their study in 2003, examined the fatigue strength of X40CrMoV5-1 hot work tool steel at different temperatures (50-600°C) and loads. In his works R.R. A Moore type rotational bending fatigue testing device was used (Yeşildal, Şen and Kaymaz, 2003).

Paepegem and Degrieck conducted scientific studies in 2001 to examine the fatigue strength of fiber-reinforced composite materials. During their experimental study, they designed a planar bending stress fatigue test device suitable for the purpose of the study. With this device they designed, bending stress was applied in one direction or in both directions, from minimum to maximum (Van Paepegem and Degrieck, 2001).

Burhan and Çavdar designed an eccentric spring fatigue test device in 2010 to examine the fatigue strength of eccentric springs. In this study, they examined the fatigue strength and shape changes of compression springs of different diameters and sizes under variable loads (Burhan and Çavdar, 2010).

In their study conducted by Küçük et al. in 2014, R.R. They designed a Moore type fatigue testing device. The designed device can reach a maximum rotation speed of 5000 rpm with the help of a 1.5Hp engine (Küçük et al., 2014).

2. Materials and Methods

2.1. Design of Fatigue Test Device

While designing the rotational bending fatigue test device, the design was started by examining the devices currently in use. The elements that can be produced in the initially designed R. R. Moore type rotational bending fatigue device were modeled in Solidworks software, taking into account the dimensions of the examined rotational bending fatigue device elements (Figure 1-Figure 3). In the next stage, the designed parts were produced.

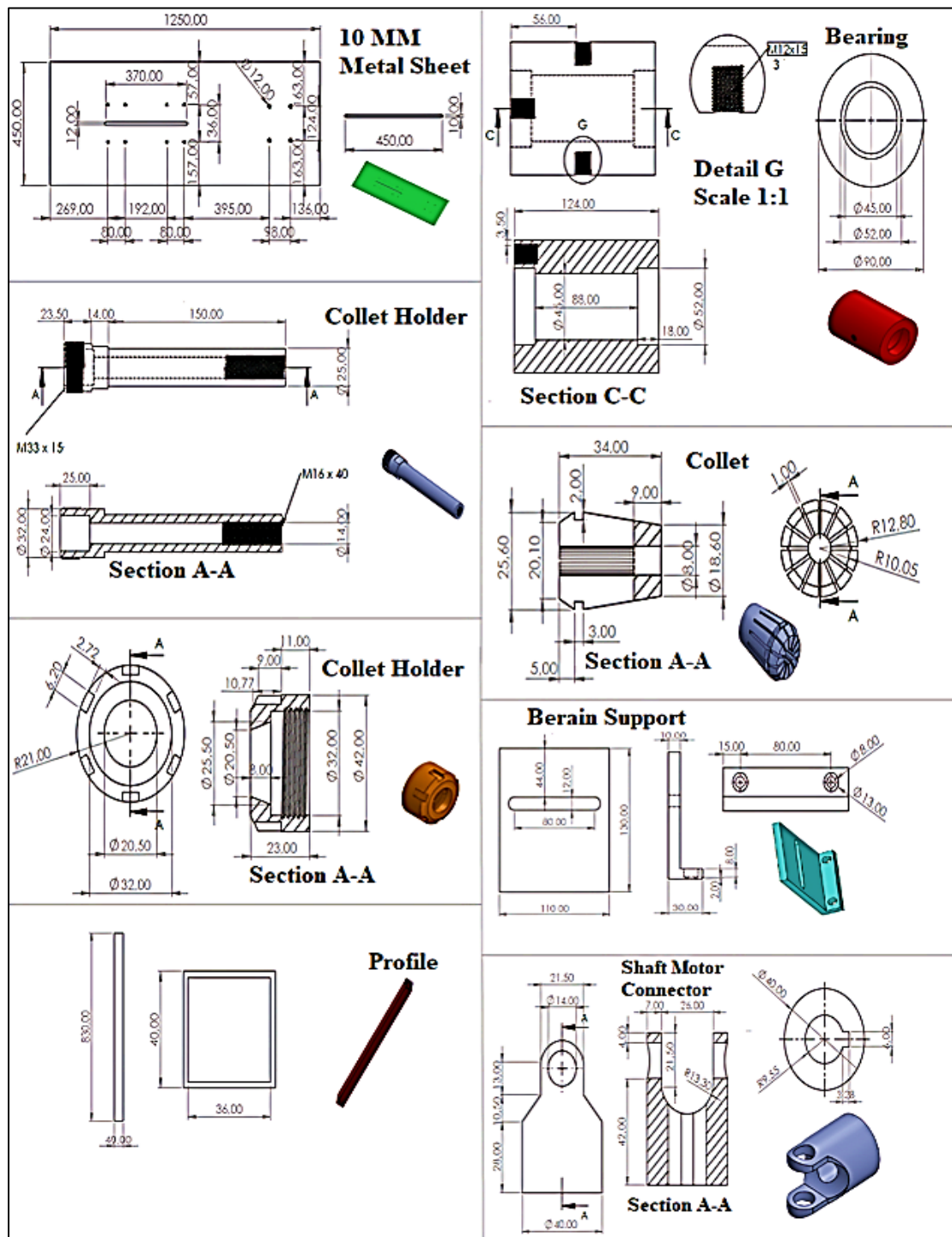


Figure 1. Technical drawing of rotational bending fatigue testing machine equipment

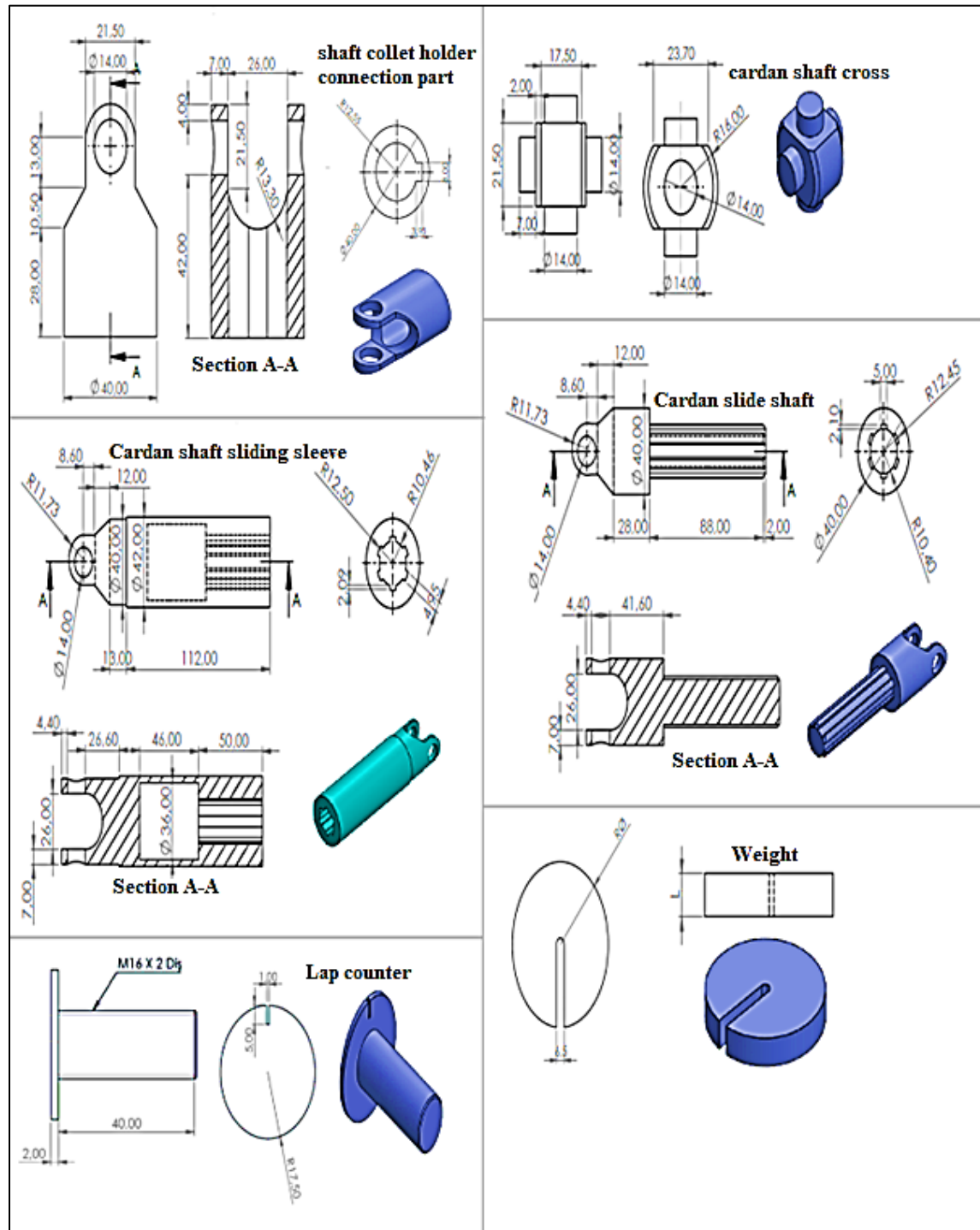


Figure 2. Technical drawing of rotational bending fatigue testing machine equipment (continued)

| Item No | Component | Material | Explanation | Amount |
|---------|------------------------------------|------------|-------------|--------|
| 1 | 10mm Metal Sheet | HARDOX 450 | Production | 1 |
| 2 | Engine | | Ready-Made | 1 |
| 3 | Bearing | C45 | Production | 2 |
| 4 | Collet Holder | ST42 | Ready-Made | 2 |
| 5 | Collet | ST42 | Ready-Made | 2 |
| 6 | Collet Nut | ST37 | Ready-Made | 2 |
| 7 | 2205 -2rs-tvh Bearing | | Ready-Made | 4 |
| 8 | Sample | AL6063-C45 | Production | 1 |
| 9 | Support Leg | HARDOX 450 | Production | 4 |
| 10 | Weight Pin | ST37 | Production | 2 |
| 11 | Weight Hook 2 | ST37 | Production | 1 |
| 12 | Box Profile | S275JOH | Production | 4 |
| 13 | Cardan Shaft Engine Bracket | ST42 | Production | 1 |
| 14 | Cardan Shaft Collet Holder Fitting | ST42 | Production | 1 |
| 15 | Cardan Shaft Cross | ST42 | Production | 2 |
| 16 | Cardan Shaft Sliding Sleeve | ST42 | Production | 1 |
| 17 | Cardan Shaft Sliding Mill | ST42 | Production | 1 |
| 18 | Imbus Bolt M8x30 | ST37 | Ready-Made | 12 |
| 19 | M8 Nut | ST37 | Ready-Made | 12 |
| 20 | Limit Switch | | Ready-Made | 1 |
| 21 | Driver | | Ready-Made | 1 |
| 22 | Lap Counter | ST37 | Production | 1 |
| 23 | Lap Counter Wedge | KESTAMIT | Production | 1 |
| 24 | Lap Timet | | Ready-Made | 1 |
| 25 | Control and Counter Circuit | | Ready-Made | 1 |
| 26 | Emergency Stop Button | | Ready-Made | 1 |
| 27 | Weight Hook 1 | ST37 | Production | 1 |
| 28 | Weight 1 | C45 | Production | 3 |
| 29 | Weight 2 | ST37 | Production | 5 |

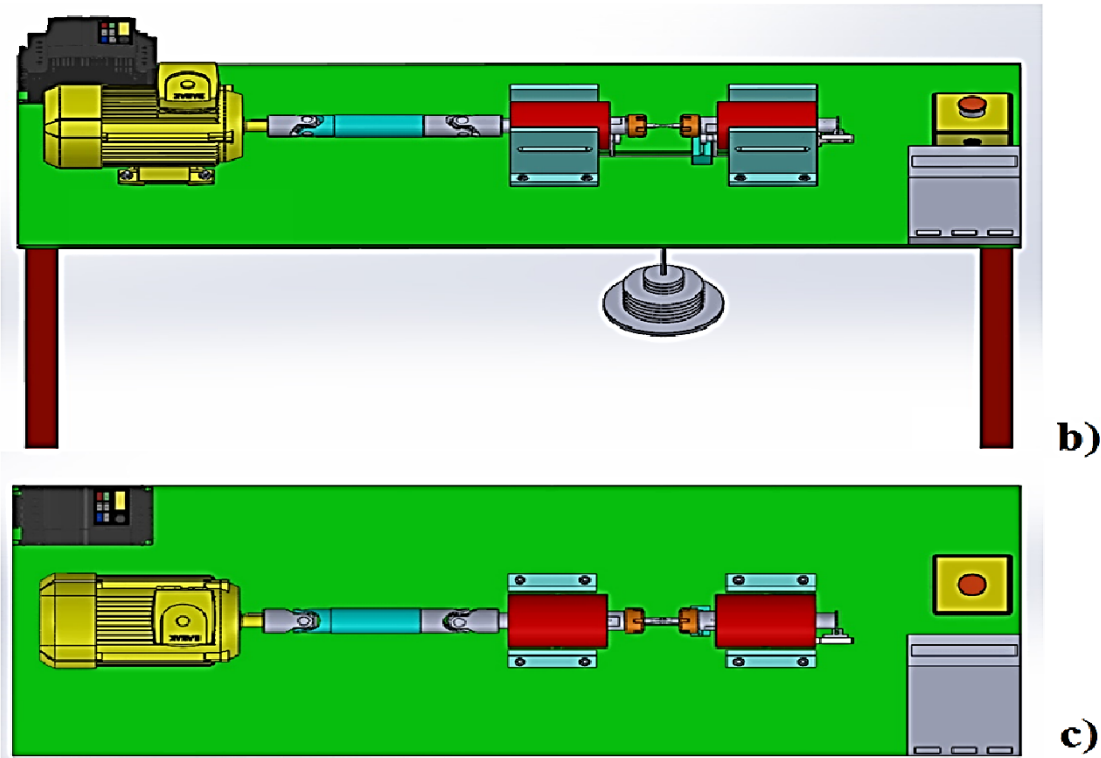
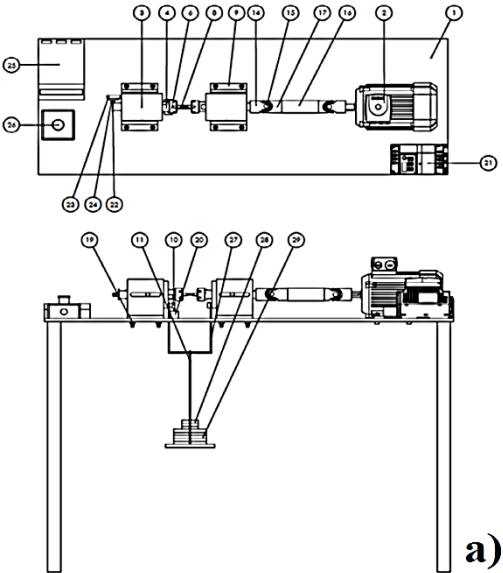


Figure 3. a. Rotational Bending Fatigue Testing Machine General Assembly Drawing b. Solidworks solid model design image front view c. Solidworks solid model design image top view

2.2. Manufacturing of Fatigue Test Device

First of all, an electric motor with a power of 1.5 Hp (1.1 Kw) and a speed of 2900 rpm was selected to provide the drive power to the system. In order for this electric motor to rotate at the desired frequency and cycle rate, a 1.5 KW 220V AC driver was connected to the electric motor. Then, it was considered to install a drill chuck or lathe chuck to connect the samples. However, considering the difficulties and loss of time in mounting the sample, this system was abandoned and it was decided to use forceps as the sample fixing element. It was decided to use ER25 collet holder, considering the different sample diameters. Thus, by changing the collet heads, samples with a diameter of 1 mm to 16 mm will be clamped. Forceps suitable for the sample diameter we will use in the experiments were selected. Studies have been carried out on systems that will transfer the rotation force from the engine to the collets. It is thought that this system should allow a rotating shaft to move in the radial direction, allowing axial misalignment to be damped. For this reason, it was decided to connect an articulated cardan shaft to the system from two opposite points. It was manufactured taking into account the cardan shaft standards. One of the joints of the cardan shaft was machined according to the diameter of the output shaft of the electric motor and a keyway was opened. The other joint of the cardan shaft was machined according to the shaft diameter of the collet holder to which it will be connected, and the keyway was opened according to the standards. A keyway was opened in the section where the collet holder will be connected to the cardan shaft, in accordance with the keyway standards, with the help of a milling cutter. Bearing selection was made by taking into account the outer diameter of the collet holder shaft and the torque of the motor. Self-aligning ball bearing was used as bearing. The reason why self-aligning ball bearings are chosen is that these types of bearings absorb axial misalignment, flexing in the shafts and housing deformations by providing angular play. In order to mount the collet holders on the lathe, two beds were made of solid C45 manufacturing steel. While making the beds, care was taken to ensure that the bed length did not exceed the length of the collet holder. The reason for this is that a part of the collet holder must remain outside in order to connect the cardan shaft to one end. The inner part of the bearings is precisely machined on a lathe according to the selected bearing diameter. Two self-aligning ball bearings have been installed on each bearing. The collet holders are inserted into these bearings and fixed with an outer circlip.

While designing the electrical hardware of the system, an electronic AC motor driver was placed that provides speed control by changing the frequency and voltage of the electric motor. Accordingly, an emergency start-stop button has been placed in the system and a circuit cut-out switch has been placed under the collet holder bed to prevent the device

from running in vain as a result of fatigue breakage. A sensor was placed on the back of the system to calculate the number of rotations (laps) during the experiment. This sensor transfers the rotation data it obtains in each revolution to an electronic digital screen. This digital display has 10 digits and can measure 1×10^9 rotations and the time passed during this period.

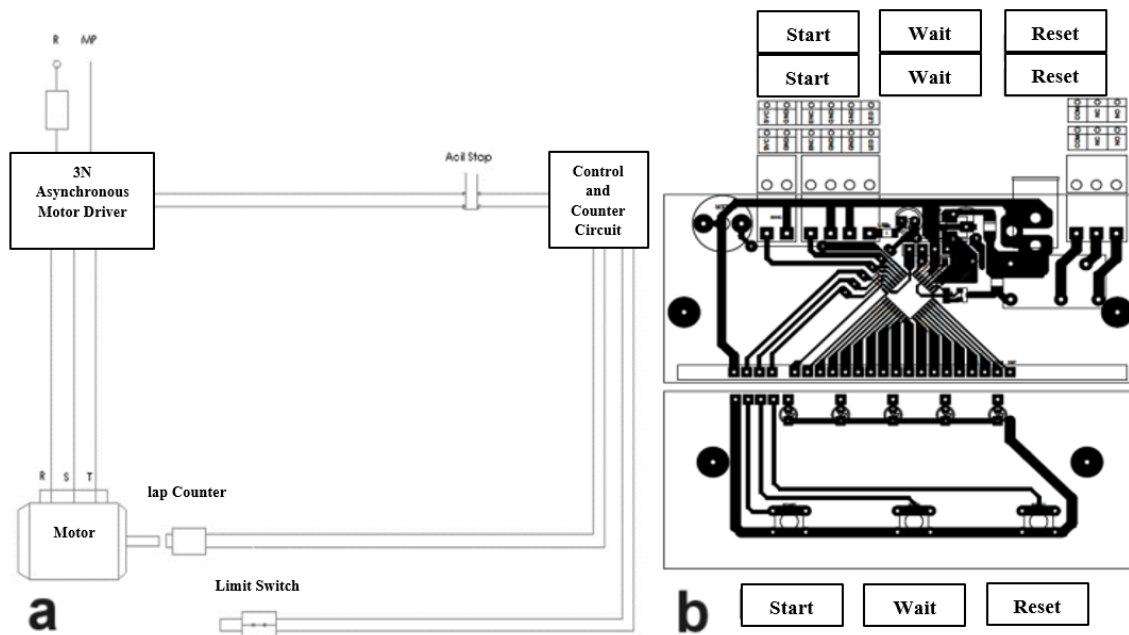


Figure 4. a. Electrical diagram of the system b. System control and counter circuit diagram

In order to start the fatigue test, the loads and moments in the system must be balanced. The loads and moments of all moving parts working together in the system were examined. The load acting on the bearing to which the cardan shaft is connected was found due to the joints. On the other bed to which the sample was attached, the load acting due to the weight of the collet clamping collar was measured. The load required to ensure moment balance of the system was calculated. The schematic representation of the load calculation is given in Figure 5.

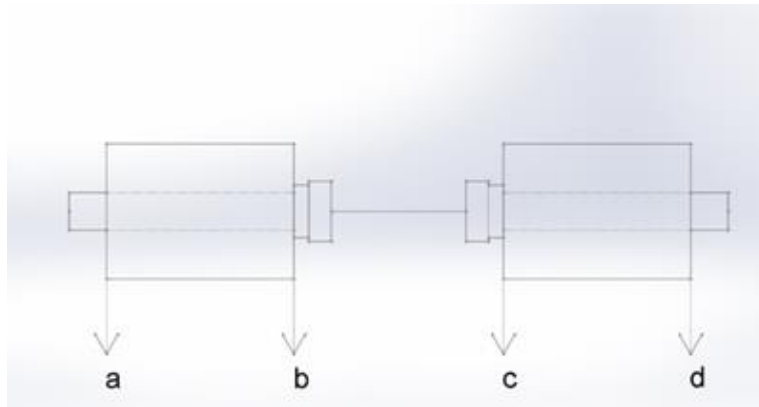


Figure 5. Loads acting on bearings

In order for the bearings to be axially balanced, the following equation must be met.

$$a - b - c + d = 0 \quad (1)$$

Here:

- a: The load exerted by the cardan shaft joint on the bearing was found to be 1700gr.
- b: The load exerted by the collet holder head on the bed was found to be 400gr.
- c: The load exerted by the collet holder head on the bed was found to be 400gr.
- d: The load applied by the lap counter sensor to the bed and was found to be 100gr.

In addition, the loads affected by the weight hook mechanism that we connected to the weight system were taken into consideration. As a result of the measurements, the load affected by the weight mechanism was found to be 184 g.

Considering the loads acting on the bearings and the weight of the weight system mechanism, as shown in the balance diagram above, the net load acting on the sample connected between two clamps will be as follows.

$1700 + 100 - 400 - 400 - 184 = 816$ gr. It will be upward.

As a result of the examinations, the system reached balance when a load weighing 816 g was connected to the weight mechanism. Studies were carried out taking this value into consideration while conducting the experiment.

2.3. Engine Type and Features

GAMAK Motor/ AGM3EL 80 M 2b / 1.1 kW / 230-400 V three-phase asynchronous motor was chosen.

Table 1. Electric Motor Specifications (www.gamak.com).

| Rated Power | | Rated Power | Velocity | Current | Power Coefficient | Efficiency | Moment | Initial Current | Initial Torque |
|-------------|-----|-------------|----------|---------|-------------------|------------|--------|-----------------|----------------|
| KW | HP | V | d/dk | A | cosØ | μ (%) | N.m | A | N.m |
| 1.1 | 1.5 | 230 | 2900 | 4,00 | 0,83 | 82,5 | 3,6 | 13,6 | 9,4 |
| 1,1 | 1,5 | 400 | 2900 | 2,30 | 0,83 | 82,7 | 3,6 | 13,6 | 9,4 |
| 1,27 | 1,7 | 460 | 3480 | 2,30 | 0,83 | 84,0 | 3,6 | 13,6 | 9,4 |

2.4. Cardan Shaft and Collet Holder Key Dimensions

In order to ensure that the thermal expansions occurring in the parts are balanced, care has been taken to use materials with similar thermal expansion coefficients. For this reason, St37 was used as the wedge material. While opening the keyways for the collet holder and cardan shaft, the keyway was opened with the help of a milling cutter by looking at the DIN 6885 keyway standards table according to the shaft diameters.

$$\sigma = \frac{16 W L D}{\pi D^3} \quad (2)$$

L: Moment arm (fixed distance between load application point and bearing support; 4 inches=101.6 mm)

σ: Stress at the outermost point of the sample

D: Minimum diameter of the sample

W: Total load applied to the sample

Instead of making separate calculations for each sample in the above equation, the coefficient value corresponding to the stress to be selected for a certain diameter value is multiplied by the W load value we calculated in Figure 6 to obtain the stress value corresponding to the load. The chart given in Figure 6 was created with the English unit system. To find the load coefficients corresponding to the diameter values of our test samples, we convert the diameter value in mm to the inch unit system. Diameter values are obtained. Then there is the load coefficient corresponding to this diameter. Here, the calculation should be made by subtracting the weights of the beds and the loading hook from the total load (Yeşildal, 1999).

| Dis. Factor | Dis. Factor | Dis. Factor | Dis. Factor | Dis. Factor | Dis. Factor | Dis. Factor | Dis. Factor |
|-------------|-------------|-------------|-------------|-------------|-------------|-------------|-------------|
| .050 .0061 | .100 .0491 | .150 .1657 | .200 .3927 | .250 .7670 | .300 1.3254 | .350 2.1046 | .400 3.1416 |
| .051 .0065 | .101 .0506 | .151 .1690 | .201 .3936 | .251 .7762 | .301 1.3387 | .351 2.1227 | .401 3.1652 |
| .052 .0069 | .102 .0521 | .152 .1723 | .202 .4046 | .252 .7855 | .302 1.3521 | .352 2.1469 | .402 3.1890 |
| .053 .0073 | .103 .0536 | .153 .1758 | .203 .4106 | .253 .7949 | .303 1.3655 | .353 2.1592 | .403 3.2128 |
| .054 .0077 | .104 .0552 | .154 .1793 | .204 .4167 | .254 .8044 | .304 1.3791 | .354 2.1776 | .404 3.2368 |
| .055 .0082 | .105 .0568 | .155 .1828 | .205 .4228 | .255 .8139 | .305 1.3928 | .355 2.1961 | .405 3.2609 |
| .056 .0086 | .106 .0585 | .156 .1864 | .206 .4291 | .256 .8235 | .306 1.4065 | .356 2.2147 | .406 3.2851 |
| .057 .0090 | .107 .0601 | .157 .1899 | .207 .4354 | .257 .8332 | .307 1.4203 | .357 2.2334 | .407 3.3094 |
| .058 .0096 | .108 .0618 | .158 .1936 | .208 .4417 | .258 .8430 | .308 1.4342 | .358 2.2523 | .408 3.3339 |
| .059 .0101 | .109 .0636 | .159 .1973 | .209 .4481 | .259 .8528 | .309 1.4482 | .359 2.2712 | .409 3.3585 |
| .060 .0106 | .110 .0653 | .160 .2010 | .210 .4546 | .260 .8628 | .310 1.4624 | .360 2.2902 | .410 3.3832 |
| .061 .0111 | .111 .0671 | .161 .2048 | .211 .4611 | .261 .8728 | .311 1.4766 | .361 2.3094 | .411 3.4079 |
| .062 .0117 | .112 .0689 | .162 .2087 | .212 .4677 | .262 .8828 | .312 1.4908 | .362 2.3286 | .412 3.4329 |
| .063 .0123 | .113 .0708 | .163 .2126 | .213 .4744 | .263 .8930 | .313 1.5052 | .363 2.3479 | .413 3.4579 |
| .064 .0129 | .114 .0727 | .164 .2165 | .214 .4811 | .264 .9032 | .314 1.5197 | .364 2.3674 | .414 3.4831 |
| .065 .0135 | .115 .0747 | .165 .2205 | .215 .4878 | .265 .9135 | .315 1.5343 | .365 2.3869 | .415 3.5084 |
| .066 .0141 | .116 .0766 | .166 .2245 | .216 .4947 | .266 .9239 | .316 1.5489 | .366 2.4066 | .416 3.5339 |
| .067 .0148 | .117 .0786 | .167 .2286 | .217 .5016 | .267 .9343 | .317 1.5637 | .367 2.4264 | .417 3.5594 |
| .068 .0154 | .118 .0807 | .168 .2328 | .218 .5086 | .268 .9449 | .318 1.5785 | .368 2.4463 | .418 3.5851 |
| .069 .0161 | .119 .0827 | .169 .2369 | .219 .5156 | .269 .9555 | .319 1.5935 | .369 2.4663 | .419 3.6109 |
| .070 .0168 | .120 .0848 | .170 .2412 | .220 .5227 | .270 .9662 | .320 1.6085 | .370 2.4864 | .420 3.6368 |
| .071 .0176 | .121 .0869 | .171 .2455 | .221 .5298 | .271 .9769 | .321 1.6236 | .371 2.5066 | .421 3.6628 |
| .072 .0183 | .122 .0891 | .172 .2498 | .222 .5371 | .272 .9878 | .322 1.6388 | .372 2.5270 | .422 3.6889 |
| .073 .0191 | .123 .0913 | .173 .2542 | .223 .5443 | .273 .9988 | .323 1.6541 | .373 2.5474 | .423 3.7153 |
| .074 .0199 | .124 .0936 | .174 .2586 | .224 .5517 | .274 1.0100 | .324 1.6696 | .374 2.5679 | .424 3.7417 |
| .075 .0207 | .125 .0959 | .175 .2631 | .225 .5591 | .275 1.0209 | .325 1.6851 | .375 2.5886 | .425 3.7682 |
| .076 .0215 | .126 .0982 | .176 .2676 | .226 .5666 | .276 1.0320 | .326 1.7006 | .376 2.6093 | .426 3.7949 |
| .077 .0224 | .127 .1005 | .177 .2722 | .227 .5742 | .277 1.0432 | .327 1.7163 | .377 2.6303 | .427 3.8217 |
| .078 .0233 | .128 .1029 | .178 .2768 | .228 .5818 | .278 1.0546 | .328 1.7321 | .378 2.6512 | .428 3.8486 |
| .079 .0242 | .129 .1054 | .179 .2815 | .229 .5895 | .279 1.0661 | .329 1.7481 | .379 2.6723 | .429 3.8755 |
| .080 .0251 | .130 .1078 | .180 .2863 | .230 .5972 | .280 1.0776 | .330 1.7641 | .380 2.6935 | .430 3.9028 |
| .081 .0261 | .131 .1103 | .181 .2911 | .231 .6051 | .281 1.0891 | .331 1.7801 | .381 2.7148 | .431 3.9301 |
| .082 .0271 | .132 .1129 | .182 .2959 | .232 .6129 | .282 1.1008 | .332 1.7963 | .382 2.7363 | .432 3.9575 |
| .083 .0281 | .133 .1155 | .183 .3008 | .233 .6209 | .283 1.1126 | .333 1.8126 | .383 2.7578 | .433 3.9850 |
| .084 .0291 | .134 .1181 | .184 .3058 | .234 .6289 | .284 1.1244 | .334 1.8289 | .384 2.7795 | .434 4.0127 |
| .085 .0301 | .135 .1208 | .185 .3108 | .235 .6370 | .285 1.1363 | .335 1.8454 | .385 2.8012 | .435 4.0405 |
| .086 .0312 | .136 .1235 | .186 .3158 | .236 .6452 | .286 1.1484 | .336 1.8620 | .386 2.8231 | .436 4.0685 |
| .087 .0323 | .137 .1262 | .187 .3210 | .237 .6535 | .287 1.1619 | .337 1.8787 | .387 2.8451 | .437 4.0968 |
| .088 .0335 | .138 .1288 | .188 .3262 | .238 .6617 | .288 1.1726 | .338 1.8955 | .388 2.8672 | .438 4.1247 |
| .089 .0346 | .139 .1318 | .189 .3314 | .239 .6701 | .289 1.1849 | .339 1.9123 | .389 2.8895 | .439 4.1530 |
| .090 .0358 | .140 .1347 | .190 .3367 | .240 .6786 | .290 1.1972 | .340 1.9293 | .390 2.9118 | .440 4.1815 |
| .091 .0370 | .141 .1376 | .191 .3420 | .241 .6871 | .291 1.2095 | .341 1.9464 | .391 2.9342 | .441 4.2100 |
| .092 .0382 | .142 .1406 | .192 .3474 | .242 .6957 | .292 1.2221 | .342 1.9635 | .392 2.9568 | .442 4.2387 |
| .093 .0395 | .143 .1435 | .193 .3529 | .243 .7043 | .293 1.2347 | .343 1.9809 | .393 2.9795 | .443 4.2676 |
| .094 .0408 | .144 .1466 | .194 .3584 | .244 .7131 | .294 1.2474 | .344 1.9982 | .394 3.0023 | .444 4.2965 |
| .095 .0421 | .145 .1497 | .195 .3639 | .245 .7219 | .295 1.2602 | .345 2.0157 | .395 3.0251 | .445 4.3256 |
| .096 .0434 | .146 .1528 | .196 .3696 | .246 .7308 | .296 1.2730 | .346 2.0333 | .396 3.0482 | .446 4.3548 |
| .097 .0448 | .147 .1559 | .197 .3753 | .247 .7397 | .297 1.2860 | .347 2.0510 | .397 3.0714 | .447 4.3842 |
| .098 .0462 | .148 .1591 | .198 .3810 | .248 .7487 | .298 1.2991 | .348 2.0687 | .398 3.0946 | .448 4.4137 |
| .099 .0476 | .149 .1624 | .199 .3868 | .249 .7578 | .299 1.3122 | .349 2.0866 | .399 3.1181 | .449 4.4433 |

Figure 6. R. R. Moore Type Fatigue Device Loading Coefficients

2.6. Preparation of Test Samples

The samples to be used in the fatigue test were machined from 8 mm diameter shafts consisting of AA 6063 aluminum alloy and C45 manufacturing steel. Shafts with a diameter of 8 mm were cut into 90 mm lengths and machined on a CNC lathe and prepared as shown in Figure 7. The dimensions of the test samples according to ASTM E-466 standards are shown in Figure 26. A total of 24 samples were prepared to test Aluminum AA 6063 samples, 3 of each weight. C45 manufacturing steel samples were prepared in the same way, a total of 27 samples to be tested, 3 of each weight. The surface roughness of the prepared samples was tried to be reduced to minimum levels with the help of 300 grit and 1200 grit sandpaper.

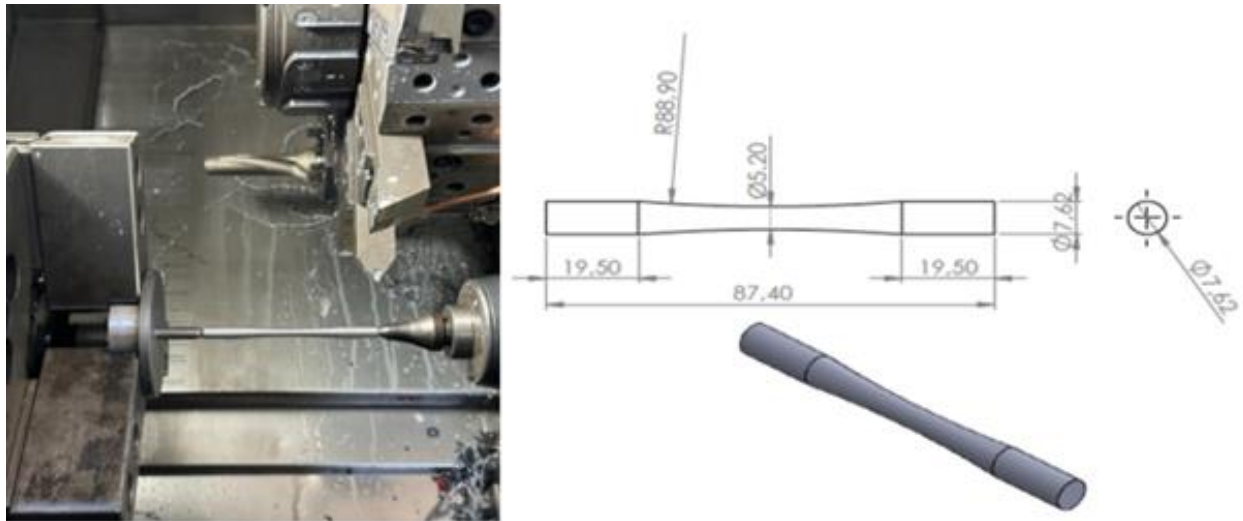


Figure 7. Fatigue test sample dimensions and processing on CNC lathe (ASTM, 2013).

2.6.1. AA 6063 Test Sample

Considering its characteristic features, Aluminum AA 6063 is a metal with high corrosion and fatigue resistance, high weldability and good cold forming properties.

Scope of application; It is used in many areas of our lives such as doors, windows, building frame systems, lamps, stairs and window railings, electronic systems, radiator systems, heat exchanger applications.

Table 2. Chemical composition [%] of AA 6063 aluminum alloy (Jayaraman, 2014).

| Fe | Si | Cu | Mn | Mg | Zn | Cr | Ti | Other |
|------|---------|-----|-----|----------|-----|-----|------|-------|
| 0.35 | 0.2-0.6 | 0.1 | 0.1 | 0.45-0.9 | 0.1 | 0.1 | 0.15 | 0.15 |

Table 3. AA 6063 aluminum alloy mechanical properties (Jayaraman, 2014).

| Temper | Yield Strength (Mpa) | Tensile Strength (Mpa) | Elongation (50%) | Hardness (Brinell) |
|--------|-------------------------|---------------------------|---------------------|-----------------------|
| 0 | 50 | 100 | 26 | 25 |
| T1 | 90 | 150 | 24 | 45 |
| T4 | 90 | 160 | 21 | 50 |
| T5 | 110-175 | 150-215 | 12 | 60 |
| T6 | 170-210 | 205-245 | 12 | 75 |
| T8 | 240 | 260 | 9 | 80 |

2.6.2. C45 Manufacturing Steel Test Sample

C45 manufacturing steel contains small amounts of elements such as manganese, sulfur, silicon and phosphorus in its structure. It is a medium tensile manufacturing steel supplied hot rolled or annealed. It has characteristics such as good machinability, high weldability, high resistance to impacts and suitable for surface hardening.

Scope of application; It is used in many engineering applications, especially in bolts, studs, vehicle axles, shaft construction, machinery and equipment.

Table 4. Chemical composition [%] of C45 manufacturing steel (Tanasković, et al., 2020).

| C | Si | Mn | P _{max} | S _{max} |
|----------|----------|---------|------------------|------------------|
| 0.42-0.5 | 0.15-0.4 | 0.5-0.8 | 0.045 | 0.045 |

Table 5. Mechanical properties of C45 Manufacturing steel (Tanasković, et al., 2020).

| Yield strength R _{p0.2%} [MPa] | Tensile strength R _m [MPa] | Elongation [%] | Toughness [J] |
|--|--|----------------|---------------|
| 325 | 500-700 | 20 | 21 |

The measurements of the samples to be used in fatigue tests were made according to sample standards and can be seen in Figure 7.

3. Results

3.1. Rotary Bending Fatigue Device Production

After the production of the parts (Figure 1-Figure 2) of which the solid model was created by designing in Solidworks software, the purchased electric motor and other electrical components were assembled as shown in Figure 8 and the device production was completed.



Figure 8. Rotational bending fatigue test device manufacturing drawing a. front view b. top view

3.2. Fatigue Tests on Rotational Bending Fatigue Device

AA 6063 and C45 fatigue samples, produced in accordance with ASTM E-466 standards, were connected to the manufactured rotational bending fatigue test device. During the connection of the samples to the forceps, care was taken to ensure that the narrowed section of the samples was in the middle of the two forceps. Three samples of each weight were tested and the time and number of turns until fatigue failure occurred in the samples were measured. The stress values corresponding to the weight applied to the samples in Table 6 and Table 7 were obtained by multiplying the applied load with the load coefficient of 0.4167, which corresponds to the 5.2 mm diameter value in Figure 6.

3.2.1. AA 6063 Aluminum Alloy Testing on Rotary Bending Fatigue Device

The stress applied to the samples and the number of turns obtained until the fatigue fracture occurs are given in Table 6.

Table 6. AA 6063 aluminum alloy fatigue test data

| Sample No | Fracture Time | Stress (N/mm ²) | Number of Fracture Rounds |
|------------|---------------|-----------------------------|---------------------------|
| Al606314-1 | 00:00:49 | 153,6475 | 2448 |
| Al606314-2 | 00:01:11 | 153,6475 | 3507 |
| Al606314-3 | 00:01:45 | 153,6475 | 5196 |
| Al606313-1 | 00:02:28 | 141,8765 | 7360 |
| Al606313-2 | 00:03:31 | 141,8765 | 10486 |
| Al606313-3 | 00:04:07 | 141,8765 | 12349 |
| Al606312-1 | 00:09:11 | 130,1054 | 27559 |

| | | | |
|------------|----------|----------|----------|
| Al606312-2 | 00:09:41 | 130,1054 | 29072 |
| Al606312-3 | 00:14:31 | 130,1054 | 43609 |
| Al606311-1 | 00:19:42 | 118,3343 | 59288 |
| Al606311-2 | 00:20:33 | 118,3343 | 59681 |
| Al606311-3 | 00:24:25 | 118,3343 | 73383 |
| Al606310-1 | 00:33:07 | 106,5633 | 99255 |
| Al606310-2 | 00:40:41 | 106,5633 | 122533 |
| Al606310-3 | 00:56:32 | 106,5633 | 170083 |
| Al606309-1 | 01:21:56 | 94,7922 | 246582 |
| Al606309-2 | 01:45:36 | 94,7922 | 317817 |
| Al606309-3 | 02:54:07 | 94,7922 | 504612 |
| Al606308-1 | 05:07:13 | 83,0212 | 921836 |
| Al606308-2 | 05:43:52 | 83,0212 | 1035594 |
| Al606308-3 | 05:51:31 | 83,0212 | 1058240 |
| Al606307-1 | 29:18:59 | 77,1356 | 5276992 |
| Al606307-2 | 66:20:09 | 71,2501 | 11951624 |
| Al606307-3 | 73:43:02 | 71,2501 | 13269113 |

A Wöhler diagram was drawn as shown in Figure 9, in line with the data obtained from the designed rotational bending fatigue test device.

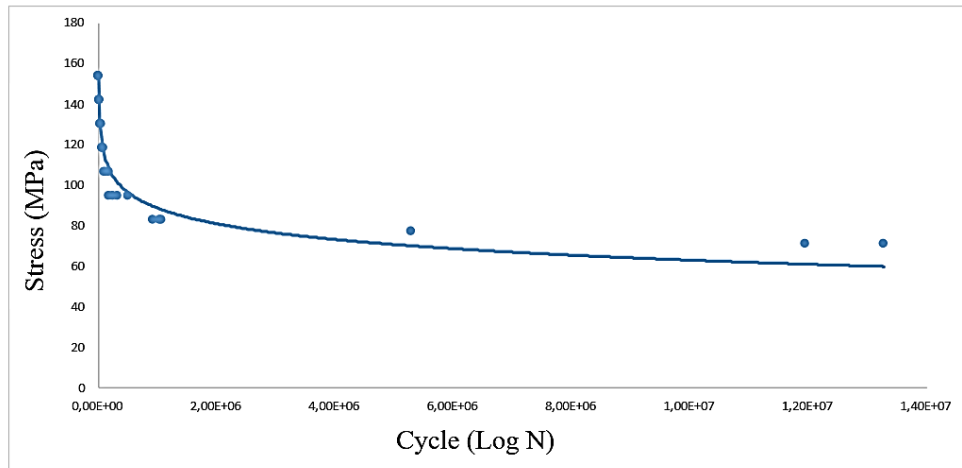


Figure 9. Aluminum AA 6063 Wöhler diagram

Figure 9 shows the comparative logarithmic S-N curves of AA 6063 aluminum alloy samples. The load was applied until the sample broke or completed $1.0\text{E}+07$ cycles. The curves showed a sharp decrease in the range of 160-80 MPa. The fatigue limit value of AA 6063 Al alloy material is determined as 71.250 MPa.

There are various studies in the literature examining the fatigue properties of AA 6063 aluminum alloys. Yahya et al. (2015) in their study; They examined the low-cycle fatigue

behavior of AA 6063-T6 alloy taken at room temperature using the strain-controlled simply supported beam test (Yahya et al., 2015).

Nanninga et al. (2010) examined the effect of routing and extrusion seam welding on the fatigue life of a milled hollow AA 6063 aluminum alloy extrusion profiles (Nanninga et al., 2010).

In his book published by Nanninga (2008) and in the light of other studies in the literature, it was found that the average fatigue limit of AA 6063 Aluminum alloy is 70 ± 10 MPa and that it does not fail up to 107 cycles below this (Nanninga, 2008).

As a result, the fatigue limit value/life value in AA 6063 Aluminum alloys obtained from hysteresis loops at different strain amplitudes is consistent with the results reported in the literature, and the cause-effect relationship has been reported by various researchers.

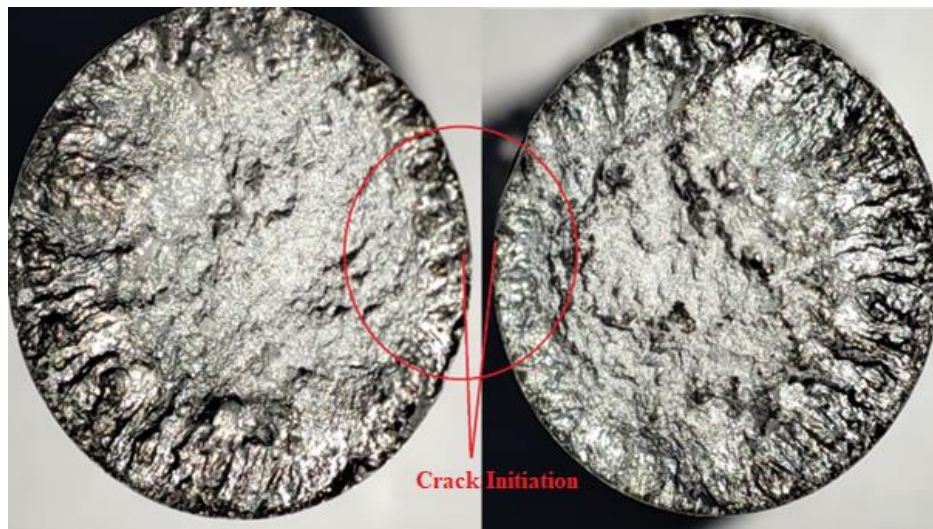


Figure 10. Fatigue damage surface image of AA 6063 Aluminum Alloy

Figure 10 shows the macro surface image of fatigue damage on two opposing fracture surfaces taken from the same AA 6063 alloy sample. The fatigue crack initiation region is circled.

In fatigue damage of aluminum alloy, macro cracks grow with the sliding of atomic planes that have low shear resistance, and shear cracks tend to progress in the parts where maximum shear stress is located. It results in the sudden breaking of the grains in the form of shear fracture under the effect of shear stresses. In this study, fatigue fracture damage occurred in this way, and features similar to the fatigue damage of AA 6063 material were observed by Patel et al. reported by (Patel et al., 2022).

3. Discussion and Conclusion

In this study, an optional R. R. Moore type rotational bending fatigue test device was designed and produced to perform fatigue tests of materials. This tester is suitable for testing circular cross-section steel, metal, aluminum, etc. with different specifications. By finding the fatigue life of samples under different loads, it allows us to graphically monitor the obtained results and findings.

Fatigue analysis was performed on the device where different loads were applied with AA 6063 aluminum alloy material and C45 manufacturing steel, and the accuracy of the production was evaluated according to the standards and results consistent with the literature studies were obtained.

4. Acknowledge

The study is related to a portion of Mustafa ÇİPİL's Master's thesis. Thanks for all valuable comments from editors and reviewers, which helped us improve the quality of the manuscript.

References

- [1] ASTM. (2013). Standard Test Methods for Tension Testing of Metallic Materials, ASTM International.
- [2] Burhan, M. ve Çavdar, K. (2010). Eksantrik yay yorulma cihazının tasarımı ve imalatı. Uludağ Üniversitesi Mühendislik Fakültesi Dergisi, 15(1).
- [3] Công, T. C., Thắng, N. V., Thủy, T. T. T., Dương, K. Đ. ve Blongher, N. (2018). Nghiên cứu sức bền mỏi của vật liệu thép C45 trước và sau khi tôi cứng Studying the fatigue strength of C45 steel material before and after quenching.
- [4] Ewing, J. A. ve Humfrey, J. C. W. (1903). VI. The fracture of metals under repeated alternations of stress. Philosophical Transactions of the Royal Society of London. Series A, Containing Papers of a Mathematical or Physical Character, 200(321-330), 241-250.

- [5] Jayaraman, P. (2014). Multi-response optimization of machining parameters of turning AA6063 T6 aluminium alloy using grey relational analysis in Taguchi method. *Procedia Engineering*, 97, 197-204.
- [6] Küçük, E., Özçelik, S., Bakacak, K.A., Sun, Y. ve Ahlatcı, H. (2014). Dönel eğmeli yorulma test cihazının tasarımı ve üretimi döner çubuk bükme yorulma test cihazı tasarım ve imalatı. I. Uluslararası Endüstriyel Tasarım Mühendisliği Sempozyumu, Karabük Üniversitesi.
- [7] Marzoli, L. M., Strombeck, A. V., Dos Santos, J. F., Gambaro, C. ve Volpone, L. M. (2006). Friction stir welding of an AA6061/Al₂O₃/20p reinforced alloy. *Composites science and technology*, 66(2), 363-371.
- [8] McAdam, D. J. ve Relationships, S. S. C. (1927). Corrosion fatigue of metals. *Journal Transaction American Society Steel Treat*, 11, 355-79.
- [9] Nanninga, N. E. (2008). High cycle fatigue of AA6082 and AA6063 aluminum extrusions. Michigan Technological University.
- [10] Nanninga, N., White, C., Mills, O. ve Lukowski, J. (2010). Effect of specimen orientation and extrusion welds on the fatigue life of an AA6063 alloy. *International journal of fatigue*, 32(2), 238-246.
- [11] Orowan, E. (1939). Theory of the fatigue of metals. *Proceedings of the Royal Society of London. Series A. Mathematical and Physical Sciences*, 171(944), 79-106.
- [12] Patel, M., Chaudhary, B., Murugesan, J., Jain, N. K. ve Patel, V. (2022). Enhancement of tensile and fatigue properties of hybrid aluminium matrix composite via multipass friction stir processing. *Journal of materials research and technology*, 21, 4811-4823.
- [13] Sayid, A. A., El-Kashif, E., Adly, M. A., Morsy, M. A. ve Abdelkawy, A. (2021). Fatigue behavior of surfaced C45 steel. *Journal of Engineering and Applied Science*, 68(1), 1-11.
- [14] Swanson, S. R. (Ed.). (1974). *Handbook of fatigue testing* (Vol. 566). ASTM International.
- [15] Tanasković, D., Arandelović, M., Đorđević, B., Jeremić, L., Sedmak, S. ve Gajin, M. (2020). Repair attempts of cold crack on forklift made of C45 steel: Case study. *Welding and Material Testing*, 29(4), 25-28.

- [16] Tauscher, H. (1983). Çelik ve dökme demirlerin yorulma dayanımı malzeme davranışı biçim etkisi ve hesaplama yöntemleri.
- [17] Teed, P. L. (1950). The properties of metallic materials at low temperatures, Vol. 1. New York.
- [18] Thompson, N. ve Wadsworth, N. J. (1958). Metal fatigue. *Advances in Physics*, 7(25), 72-169.
- [19] Uçan R. ve Topuz A., (1991). 36Mn5 Çeliğinde yorulma kırılma tokluğunun ve çatlak ilerleme parametrelerinin belirlenmesi. Üçüncü ulusal kırılma konferansı, İTÜ.
- [20] Van Paepegem, W. ve Degrieck, J. (2001). Experimental set-up for and numerical modelling of bending fatigue experiments on plain woven glass/epoxy composites. *Composite structures*, 51(1), 1-8.
- [21] Yahya, M. M., Mallik, N. ve Chakrabarty, I. (2015). Low cycle fatigue (LCF) behavior of AA6063 aluminium alloy at room temperature. *Int. J. Emerging Adv. Res. Technol.*, 5, 100.
- [22] Yeşildal, R. (1999). X40CrMoV 5 1 sıcak iş takım çeliğinin yüksek sıcaklık yorulma mukavemetinin incelenmesi. Atatürk Üniversitesi, Erzurum.
- [23] Yeşildal, R., Şen S. ve Kaymaz, İ. (2003). X40CrMo 5 1 Çeliğinin 20-600oC Arasındaki Yorulma Davranışı. *Dokuz Eylül Üniversitesi Mühendislik Fakültesi Fen ve Mühendislik Dergisi*, 5(1), 159-171.